

## Pseudo-Depth/Intercept-Time Monotonicity Requirements in the Inverse Scattering Algorithm for Predicting Internal Multiple Reflections

Bogdan G. Nita<sup>1,\*</sup> and Arthur B. Weglein<sup>2</sup>

<sup>1</sup> *Department of Mathematical Sciences, Montclair State University, 1 Normal Avenue, Montclair, NJ 07043, USA.*

<sup>2</sup> *Department of Physics, University of Houston, 617 Science and Research Bldg. 1, Houston, TX 77004, USA.*

Received 28 January 2008; Accepted (in revised version) 22 May 2008

Communicated by Lianjie Huang

Available online 15 July 2008

---

**Abstract.** In this paper we discuss the inverse scattering algorithm for predicting internal multiple reflections (reverberation artefacts), focusing our attention on the construction mechanisms. Roughly speaking, the algorithm combines amplitude and phase information of three different arrivals (sub-events) in the data set to predict one multiple reflection. The three events are conditioned by a certain relation which requires that their pseudo-depths, defined as the depths of their turning points relative to the constant background velocity, satisfy a lower-higher-lower relationship. This implicitly assumes a pseudo-depth monotonicity condition, i.e., the relation between the actual depths and the pseudo-depths of any two sub-events is the same. We study this relation in pseudo-depth and show that it is directly connected with a similar relation between the vertical or intercept times of the sub-events. The paper also provides the first multidimensional analysis of the algorithm (for a vertically varying acoustic model) with analytical data. We show that the construction of internal multiples is performed in the plane waves domain and, as a consequence, the internal multiples with headwaves sub-events are also predicted by the algorithm. Furthermore we analyze the differences between the time monotonicity condition in vertical or intercept time and total travel time and show a 2D example which satisfies the former but not the latter. Finally we discuss one case in which the monotonicity condition is not satisfied by the sub-events of an internal multiple and discuss ways of lowering these restrictions and of expanding the algorithm to address these types of multiples.

**AMS subject classifications:** 86A22, 35P25, 86-08

**Key words:** Multiple reflections, seismic imaging, inverse scattering.

---

\*Corresponding author. *Email addresses:* nitab@mail.montclair.edu (B. G. Nita), aweglein@uh.edu (A. B. Weglein)

## 1 Introduction

The inverse scattering series is presently the only multidimensional method for inverting for the properties of an unknown medium without adequate information about that medium. When the series converges it achieves full inversion given the whole data set (including free surface reverberations and internal multiple reflections) and information about a chosen reference medium. Carvalho [6] tested numerically the convergence properties of the full inverse scattering series and found that the series converges only for limited contrast between the actual and the reference medium of choice. In the '90's, Weglein and collaborators developed the subseries method (for a history and description see [18]) which consists in identifying specific subseries in the full series, which perform targeted tasks with better convergence properties than the whole series. These subseries were imagined to be a sequence of steps, similar to the processing steps undertaken in geophysical exploration, which would achieve

1. Free surface multiple elimination;
2. Internal multiple elimination;
3. Imaging in depth;
4. Inversion for the medium properties.

It is reasonable to assume, and experience showed this assumption to be true, that since the full series only requires data and information about a reference medium to invert, the same holds for any of the four specific subseries.

The inverse scattering series, and the subsequent task specific subseries, assume that the input data satisfies several pre-requisites. First, it is assumed that the source signature or wavelet has been deconvolved from the data. Second, both the source and receiver ghosts (the part of the wavefield which travels from the source to the free surface and from the free surface to the receiver) have been eliminated from the collected data. Third, the collected data itself has an appropriate sampling or the data reconstruction algorithms are able to improve the acquisition sampling to an appropriate degree. When these prerequisites are not satisfied, the algorithms derived from this method will reach incorrect conclusions/results, e.g., false or no prediction of free-surface and internal multiples, incorrect location of subsurface structures, errors in parameter estimation. Last but not least we mention that the algorithms are derived from a point-source point-receiver wave theory approach and any deviations from that, e.g., source and receiver arrays, would have to be studied to understand how they affect the algorithms.

In 1994, Araujo [2] identified the first term in the subseries for internal multiple elimination (see also [17]). This first term by itself exactly predicts the time of arrival, or phase, and well approximates the amplitude of internal multiples, without being larger than the actual amplitude, and hence it represents an algorithm for *attenuation*. Weglein et al. [18] described the application of the algorithm to 1D analytic and 2D synthetic data. Field data tests were also performed showing an extraordinary ability to predict difficult

interbed multiples, e.g. superimposed primary and multiple etc., where other methods have failed.

The inverse scattering internal multiple attenuation algorithm was found through a combination of simple 1D models testing/evaluation and certain similarities between the way the data is constructed by the forward scattering series and the way arrivals in the data are processed by the inverse scattering series. This connection between the forward and the inverse series was analyzed and described by Matson [10, 11] and Weglein et al. [17, 18]. Specifically, they showed that an internal multiple in the forward scattering series is constructed by summing certain types of scattering interactions which appear starting with the third order in the series. The piece of this term representing the first order approximation to an internal multiple is exactly the one for which the point scatterers satisfy a certain lower-higher-lower relationship in actual depth. Summing over all interactions of this type in the actual medium results in constructing the first order approximation to an internal multiple. By analogy, it was inferred that the first term in the subseries for eliminating the internal multiples would be one constructed from events satisfying the same lower-higher-lower relationship in pseudo-depth. The assumption that the ordering of the actual and the pseudo depths of two sub-events is preserved, i.e.

$$z_1^{actual} < z_2^{actual} \iff z_1^{pseudo} < z_2^{pseudo}, \quad (1.1)$$

has been subsequently called “the pseudo-depth monotonicity condition”.

In this paper we further analyze this relation and show that it is equivalent to a vertical or intercept time (here denoted by  $\tau$ ) monotonicity condition

$$z_1^{actual} < z_2^{actual} \iff \tau_1 < \tau_2, \quad (1.2)$$

for any two sub-events. We also look at the differences between the time monotonicity condition in vertical or intercept time and total travel time. The latter was pointed out by a different algorithm derived from the inverse scattering series by ten Kroode [8] and further described by Malcolm and de Hoop [9]. We show a 2D example which satisfies the time monotonicity in vertical or intercept time (and hence is predicted by the original algorithm) but not in total travel time. Finally we discuss a case in which the monotonicity condition is not satisfied by the sub-events of certain internal multiple reflection in either vertical or total travel time and consequently the multiple will not be predicted by either one of the two algorithms. For these cases, the monotonicity condition turns out to be too restrictive and we discuss ways of lowering these restrictions and hence expanding the algorithm to address these types of multiples.

In Section 2 we will describe the relationship between internal reverberations and scattering theory with special focus on the inverse scattering algorithm for predicting them. A 1.5D example is analyzed in Section 3 with analytical data where internal multiples with headwaves sub-events are shown to be predicted by the algorithm. We further look in Sections 4 and 5 at several 2D examples to better understand the relationship between the sub-events which are used by the algorithm to construct the phase and the

amplitude of the internal multiple. Some comments and conclusions are presented in the last section.

## 2 Internal multiple reflections and their relation with scattering theory

Internal multiple reflections are easier to understand than they are to define. In fact, their definition started off as a simple concept - a wave event having two or more upward reflection and one or more internal (i.e. not at the free surface) downward reflections - and evolved to more complicated and precise notions (for a description of these concepts see [19]). This evolution was driven by the development of higher understanding of wave propagation and that of better models of complex media in seismic applications. Recently, Weglein and Dragoset [19] have introduced more general definitions and designations for primary and multiply reflected events, namely prime and composite events. According to those definitions, a *prime event* is not decomposable into other recorded events such that those sub-event ingredients combine by adding and/or subtracting time of arrival to produce the prime. A *composite event* is composed of sub-events that combine in the above described manner to produce the event. These definitions, which generalize all the previous ones, and the notion of sub-events, were suggested by the inverse scattering internal algorithm which is going to be discussed in this section. One notable difference between these new concepts and the classical ones is that they do not make any inferences about, or references to the medium or to the history of the recorded wave event. The entire decision whether or not an event in the data is a single or a multiple reflection is based on the information contained in that data set itself. In the next few paragraphs we introduce the mathematical foundation for the forward and the inverse scattering theory with a special focus on how internal multiple reflections relate to them.

The differential equations describing wave propagation in an actual and a reference medium can be written as

$$\mathbf{L}\mathbf{G} = -\mathbf{I} \quad (2.1)$$

and

$$\mathbf{L}_0\mathbf{G}_0 = -\mathbf{I}, \quad (2.2)$$

where  $\mathbf{L}$ ,  $\mathbf{L}_0$  and  $\mathbf{G}$ ,  $\mathbf{G}_0$  are the actual and reference differential and Greens operators, respectively, for a single temporal frequency and  $\mathbf{I}$  is the identity operator. Eqs. (2.1) and (2.2) assume that the source and receiver signatures have been deconvolved. The perturbation,  $\mathbf{V}$ , and the scattered field operator,  $\psi_s$ , are defined as

$$\mathbf{V} = \mathbf{L} - \mathbf{L}_0, \quad (2.3)$$

$$\psi_s = \mathbf{G} - \mathbf{G}_0. \quad (2.4)$$

The fundamental equation of scattering theory, the Lippmann-Schwinger equation, relates  $\psi_s$ ,  $\mathbf{G}_0$ ,  $\mathbf{V}$  and  $\mathbf{G}$  (see, e.g., [15])

$$\psi_s = \mathbf{G} - \mathbf{G}_0 = \mathbf{G}_0 \mathbf{V} \mathbf{G}. \quad (2.5)$$

This equation can be expanded in an infinite series by repeatedly substituting  $\mathbf{G} = \mathbf{G}_0 - \mathbf{G}_0 \mathbf{V} \mathbf{G}$  into the right hand side to obtain

$$\psi_s \equiv \mathbf{G} - \mathbf{G}_0 = \mathbf{G}_0 \mathbf{V} \mathbf{G}_0 + \mathbf{G}_0 \mathbf{V} \mathbf{G}_0 \mathbf{V} \mathbf{G}_0 + \dots. \quad (2.6)$$

This series constructs the scattered field operator  $\psi_s$  as a series of terms formed as propagations in the reference medium ( $\mathbf{G}_0$ ) and interactions with the inhomogeneity ( $\mathbf{V}$ ). Notice that the scattered field is constructed everywhere, i.e. inside and outside the actual medium; when this equation is restricted to a pre-defined measurement surface, this quantity represents the recorded data and hence the equation describes a modeling procedure or a direct (forward) problem.

The perturbation operator  $\mathbf{V}$  can be expanded as a formal series

$$\mathbf{V} = \mathbf{V}_1 + \mathbf{V}_2 + \mathbf{V}_3 + \dots, \quad (2.7)$$

where  $\mathbf{V}_n$  is the portion of  $\mathbf{V}$  that is  $n$ th order in the data,  $D$ . Introducing the expression for  $\mathbf{V}$  from Eq. (2.7) into the forward series in Eq. (2.6) to find

$$\begin{aligned} \Psi_s = & \mathbf{G}_0(\mathbf{V}_1 + \mathbf{V}_2 + \dots)\mathbf{G}_0 + \mathbf{G}_0(\mathbf{V}_1 + \mathbf{V}_2 + \dots)\mathbf{G}_0(\mathbf{V}_1 + \mathbf{V}_2 + \dots)\mathbf{G}_0 \\ & + \mathbf{G}_0(\mathbf{V}_1 + \mathbf{V}_2 + \dots)\mathbf{G}_0(\mathbf{V}_1 + \mathbf{V}_2 + \dots)\mathbf{G}_0(\mathbf{V}_1 + \mathbf{V}_2 + \dots)\mathbf{G}_0 \\ & + \dots. \end{aligned} \quad (2.8)$$

Evaluating this equation on the measurement surface we notice that the left hand side represents the data itself, while the right hand side is a series in different orders of the data. By equating the coefficients of the same degree from both sides of the equation we find the system of equations

$$\begin{aligned} (\Psi_s)_m = D &= (\mathbf{G}_0 \mathbf{V}_1 \mathbf{G}_0)_m, \\ 0 &= (\mathbf{G}_0 \mathbf{V}_2 \mathbf{G}_0)_m + (\mathbf{G}_0 \mathbf{V}_1 \mathbf{G}_0 \mathbf{V}_1 \mathbf{G}_0)_m, \\ 0 &= (\mathbf{G}_0 \mathbf{V}_3 \mathbf{G}_0)_m + (\mathbf{G}_0 \mathbf{V}_1 \mathbf{G}_0 \mathbf{V}_2 \mathbf{G}_0)_m + (\mathbf{G}_0 \mathbf{V}_2 \mathbf{G}_0 \mathbf{V}_1 \mathbf{G}_0)_m + (\mathbf{G}_0 \mathbf{V}_1 \mathbf{G}_0 \mathbf{V}_1 \mathbf{G}_0 \mathbf{V}_1 \mathbf{G}_0)_m, \\ &\vdots \end{aligned} \quad (2.9)$$

where the subscript  $m$  indicates that the quantities are calculated on the measurement surface. The first of these equations can be solved for  $\mathbf{V}_1$  which in turn can be used in the second equation to solve for  $\mathbf{V}_2$  and so on. Each step requires only the recorded data  $D$  and the knowledge of the reference medium Green's function  $\mathbf{G}_0$ . When the inverse scattering series, given in Eq. (2.7), converges it achieves full inversion for the

actual medium's structure and properties from recorded data and reference medium's properties only.

The subseries method was developed by Weglein and collaborators (for a history, description and the current state see [18]) to overcome possible convergence issues of the full series. Subseries were sought for certain specific tasks corresponding to steps in seismic processing for hydrocarbon exploration: 1. free surface reverberation elimination 2. internal multiple reflections elimination 3. imaging and 4. inversion. Each step assumes that the previous ones were successful and that the problem is being restarted with a new data set; for example the imaging step assumes that all the multiple reflections (free surface or internal) were eliminated and the new data set only contains prime events. In this paper we study the algorithm developed from the inverse scattering series to predict and attenuate internal multiple reflections (task 2).

The first term in an algorithm that would process (attenuate or eliminate) internal multiples in the recorded data appears as a piece of  $\mathbf{V}_3$  (see [17, 18]) and it has the form

$$b_3(k_g, k_s, \omega) = \frac{1}{(2\pi)^2} \int_{-\infty}^{\infty} \int_{-\infty}^{\infty} dk_1 e^{-iq_1(\epsilon_g - \epsilon_s)} dk_2 e^{iq_2(\epsilon_g - \epsilon_s)} \int_{-\infty}^{\infty} dz_1 e^{i(q_g + q_1)z_1} b_1(k_g, k_1, z_1) \\ \times \int_{-\infty}^{z_1} dz_2 e^{i(-q_1 - q_2)z_2} b_1(k_1, k_2, z_2) \int_{z_2}^{\infty} dz_3 e^{i(q_2 + q_s)z_3} b_1(k_2, k_s, z_3), \quad (2.10)$$

where  $\epsilon_s$  and  $\epsilon_g$  are the source and receiver depths respectively and where  $z_1 > z_2$  and  $z_2 < z_3$  and  $b_1$  is defined in terms of the original data with free surface multiples eliminated,  $D'$ , to be

$$D'(k_g, k_s, \omega) = (-2iq_s)^{-1} B(\omega) b_1(k_g, k_s, q_g + q_s) \quad (2.11)$$

with  $B(\omega)$  being the source signature. Here  $k_s$  and  $k_g$  are horizontal wavenumbers, for source and receiver coordinates  $x_s$  and  $x_g$ , and  $q_g$  and  $q_s$  are the vertical wavenumbers associated with them. The  $b_3$  on the left hand side represents the first order prediction of the internal multiples. An internal multiple in  $b_3$  is constructed through the following procedure.

The deconvolved data without free-surface multiples in the space-time domain,  $D(x_s, x_g, t)$  can be described as a sum of Dirac delta functions

$$D(x_s, x_g, t) = \sum_a R_a \delta(t - t_a) \quad (2.12)$$

representing different arrivals (primaries and internal multiples). Here  $R_a$  represents the amplitude of each arrival and it is a function of source and receiver position  $x_s$  and  $x_g$  and frequency  $\omega$ . When transformed to the frequency domain the transformed function  $D(x_s, x_g, \omega)$  is a sum

$$\tilde{D}(x_s, x_g, \omega) = \sum_a \tilde{R}_a e^{-i\omega t_a}. \quad (2.13)$$

Here  $t_a$  is the total travel time for each arrival and it can be thought of as a sum of vertical and horizontal times  $t_a = \tau_a + t_{xa}$  (see, e.g., [7, 16]), where  $t_{xa}$  is a function of  $x_g$  and  $x_s$ . After Fourier transforming over  $x_s$  and  $x_g$ , the data is  $\tilde{D}(k_s, k_g, \omega)$ . The transforms act on the amplitude as well as on the phase of the data and transform the part of the phase which is described by the horizontal time  $t_{xa}$ . Hence  $D(k_s, k_g, \omega)$  can now be thought of as a sum of terms containing  $e^{i\omega\tau_a}$  with  $\tau_a$  being the vertical or intercept time of each arrival

$$\tilde{D}(k_s, k_g, \omega) = \sum_a \tilde{R}'_a e^{-i\omega\tau_a} \quad (2.14)$$

and where  $\tilde{R}'_a$  is the double Fourier transform over  $x_g$  and  $x_s$  of  $\tilde{R}_a e^{-i\omega t_{xa}}$ . The multiplication by the obliquity factor,  $2iq_s$ , changes the amplitude of the plane wave components without affecting the phase; hence  $b_1(k_s, k_g, \omega)$  represents an effective plane wave decomposed data and is given by

$$b_1(k_s, k_g, \omega) = \sum_a \tilde{R}''_a e^{-i\omega\tau_a}, \quad (2.15)$$

where  $\tilde{R}''_a = 2iq_s \tilde{R}'_a$  and whose phase,  $e^{-i\omega\tau_a}$ , contains information only about the recorded *actual* vertical or intercept time.

Notice that for each planewave component of fixed  $k_s$ ,  $k_g$  and  $\omega$  we have

$$\omega\tau_a = k_z^{actual} z_a^{actual}, \quad (2.16)$$

where  $k_z^{actual}$  is the actual, velocity dependent, vertical wavenumber and  $z_a^{actual}$  is the actual depth of the turning point of the planewave. Since the velocity of the actual medium is assumed to be unknown, this relationship is written in terms of the reference velocity as

$$\omega\tau_a = k_z z_a, \quad (2.17)$$

where  $k_z$  is the vertical wavenumber of the planewave in the reference medium,

$$k_z = \sqrt{\frac{\omega}{c_0} - k_s} + \sqrt{\frac{\omega}{c_0} - k_g},$$

and  $z_a$  is the pseudo-depth of the turning point. This implicit operation in the algorithm is performed by denoting  $b_1(k_s, k_g, \omega) = b_1(k_s, k_g, k_z)$  with the latter having the expression

$$b_1(k_s, k_g, k_z) = \sum_a \tilde{R}''_a e^{-ik_z z_a}. \quad (2.18)$$

The next step is to Inverse Fourier Transform over the reference  $k_z$  hence obtaining

$$b_1(k_s, k_g, z) = \int_{-\infty}^{\infty} e^{ik_z z} b_1(k_s, k_g, k_z) dk_z. \quad (2.19)$$

Putting together Eqs. (2.18) and (2.19) we find

$$b_1(k_s, k_g, z) = \sum_a \int_{-\infty}^{\infty} \tilde{R}''_a e^{ik_z(z-z_a)} dk_z \quad (2.20)$$

which represents a sum of delta-like events placed at pseudo-depths  $z_a$  and hence the  $b_1$  from the last equation is actually  $b_1(k_s, k_g, z_a)$ . This last step can also be interpreted as a downward continuation on both source and receiver sides, with the reference velocity  $c_0$ , and an imaging with  $\tau = 0$ , or, in other words, an un-collapsed F-K migration (see, e.g., [13, 14]). A discussion of differences in imaging with  $\tau$  and with  $t$  was given by Nita and Weglein [12]. Each internal multiple is constructed by considering three effective data sets  $b_1$  and searching, in the horizontal-wavenumber–pseudo-depth domain, for three arrivals which satisfy the lower-higher-lower relationship in their pseudo-depths, i.e.,  $z_1 > z_2 < z_3$ , (see Fig. 1 for an example of three such primary events). Having found such three arrivals in the data, the algorithm combines their amplitudes and phases to construct a multiple by adding the phases of the two pseudo-deeper events and subtracting the one of the pseudo-shallower ones and by multiplying their amplitudes. One can then see (see, e.g., [18]) that the time of arrival of an internal multiple is exactly predicted and its amplitude is well approximated by this procedure.

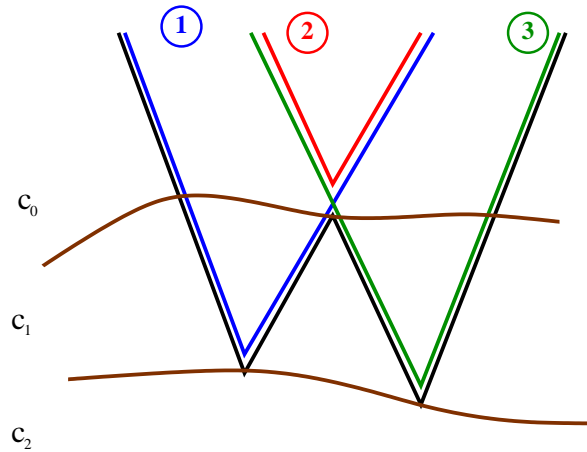


Figure 1: The sub-events of an internal multiple: the single reflections 1, 2 and 3 are arrivals in the data which satisfy the lower-higher-lower relationship in pseudo-depths  $z$ . The algorithm will construct the phase of the internal multiple (W shaped) by adding the phases of the deeper single reflections and subtracting the one of the shallow single reflection. The velocities for the three layers are represented by  $c_0$ ,  $c_1$  and  $c_2$ .

As pointed out in the first section, the lower-higher-lower restriction was inferred from the analogy with the forward scattering series description of internal multiples: the first order approximation to an internal multiple (which occurs in the third term of the series) is built up by summing over all scattering interactions which satisfy a lower-higher-lower relationship in actual depth. The assumption that this relationship is preserved in going from actual depth to pseudo-depth is called “the pseudo-depth monotonicity

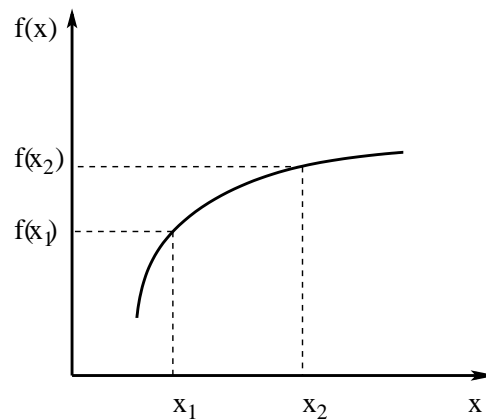


Figure 2: A monotonic function.

condition". (Recall that a monotonic function  $f(x)$  satisfies  $f(x_1) < f(x_2) \iff x_1 < x_2$ , see also Fig. 2; here, we regard the pseudo-depth as a function of actual depth). Notice that the lower-higher-lower relationship in pseudo-depth can be translated, from Eq. (2.17), in a similar longer-shorter-longer relationship in the vertical or intercept time of the three events. Accordingly, the pseudo-depth monotonicity is also translated in a vertical time monotonicity condition. Notice that this is different from the total time monotonicity assumed by the algorithm introduced by ten Kroode [8]. The latter is employing asymptotic evaluations of certain Fourier integrals which result in an algorithm in the space domain, having a ray theory assumption and the less inclusive total time monotonicity requirement. The justification for this approach was the attempt to attenuate a first order approximation to an internal multiple built by the forward scattering series. In contrast, the original scattering series algorithm is aimed at predicting and attenuating the actual multiples in the data and hence it takes into consideration the full wavefield, with no asymptotic compromises, and results in a more inclusive vertical time monotonicity condition. In Section 4 we discuss a 2D example in which the geometry of the subsurface leads to the existence of a multiple which satisfies the pseudo-depth/vertical-time but not the total time monotonicity condition.

In the next section we analyze a simple 1.5D example and show analytically how it predicts internal multiples by putting together amplitude and phase information from arrivals in the data satisfying the above condition. During this analysis we also show that the internal multiples with headwaves sub-events are attenuated by the algorithm.

### 3 Attenuation of internal multiples with headwaves sub-events: A 1.5D example

The model in this experiment is a 1D medium with the wavefield propagating in a 2D space. We consider one of the simplest cases which allow the existence of internal mul-

triples, namely one layer between two semi-infinite half-spaces separated by horizontal interfaces (see Fig. 3). The velocity only varies across the interfaces located at  $z = z_a$  and  $z = z_b$  and has the values  $c_0$ ,  $c_1$  and  $c_2$  respectively. The sources and receivers are located at the same depth  $z = 0$ . The data for such a model is given in the frequency  $\omega$  domain by (see e.g. [1])

$$D(x_h, 0; \omega) = \frac{1}{2\pi} \int_{-\infty}^{\infty} dk_h \frac{R_{01} + T_{01} R_{12} T_{10} e^{iv_1(z_b - z_a)} + \dots}{iq_s} e^{ik_h x_h} e^{ik_z z_a}, \quad (3.1)$$

where  $k_z = q_g + q_s$ ,  $k_h = k_g + k_s$ ,  $x_h = (x_g - x_s)/2$  and  $v_1 = q_{1g} + q_{1s}$ . The reflection and transmission coefficients at the corresponding interfaces  $R_{01}$ ,  $T_{01}$ ,  $R_{12}$  and  $T_{10}$  are all functions of  $k_h$  and  $\omega$ . Only the primaries from the top and the bottom interfaces are written out explicitly in this equation; the dots “...” stand for other multiple arrivals. For simplicity we will drop the writing of the dots for the rest of this example; this will effect in the prediction of the first order internal multiple only.

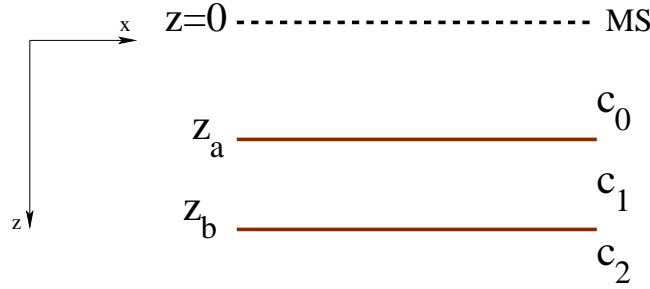


Figure 3: The model for the 1.5D example. The positive  $z$  direction points downward; the depths of the two interfaces are  $z_a$  and  $z_b$ ;  $c_0$ ,  $c_1$  and  $c_2$  are the velocities in the corresponding layers;  $MS$  denotes the measurement surface.

Notice that the expression (3.1) represents both pre-critical and post-critical arrivals, as well as, for large offsets, headwaves along both interfaces. For a discussion of how to obtain the headwaves solutions from integrating Eq. (3.1) see e.g. Aki and Richards [1] Chapter 6. The first order internal multiple that we seek to predict has the expression

$$IM_{actual}^{1st}(x_h, 0; \omega) = \frac{1}{2\pi} \int_{-\infty}^{\infty} dk_h \frac{T_{01} R_{12}^2 T_{10} R_{10} e^{2iv_1(z_b - z_a)}}{iq_s} e^{ik_h x_h} e^{ik_z z_a}. \quad (3.2)$$

This analytic formula contains both small and large offsets first order internal multiples arrivals including the multiples containing headwaves along the second interface as sub-events.

Fourier transforming the data given by Eq. (3.1) over the offset coordinate  $x_h$  and the midpoint coordinate  $x_m$  we find

$$D(k_h, 0; \omega) = \frac{R_{01} + T_{01} R_{12} T_{10} e^{-iv_1(z_b - z_a)}}{iq_s} e^{-ik_z z_a} \delta(k_g - k_s). \quad (3.3)$$

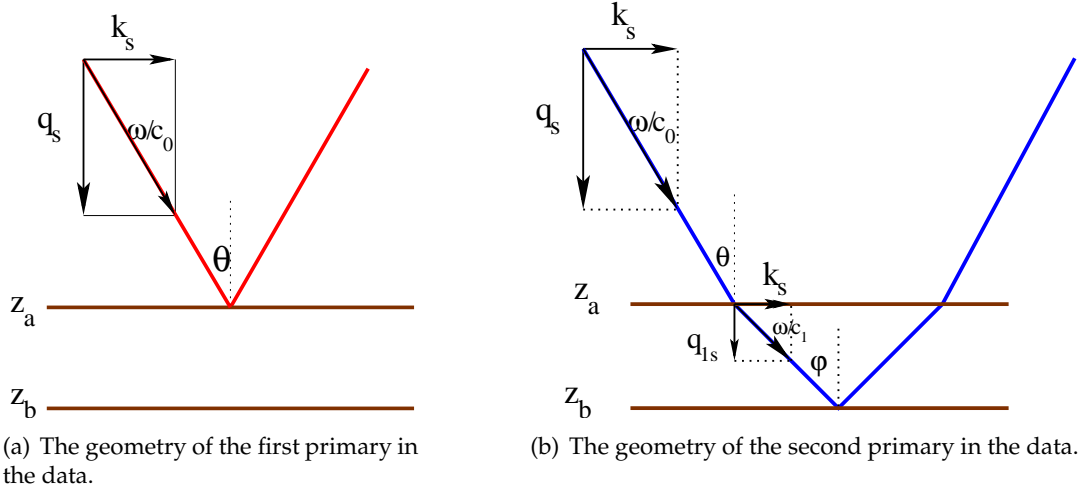


Figure 4: Geometrical representation of the two primaries.

Then  $b_1(k_h, 0; \omega) = iq_s D(k_h, 0; \omega)$  is

$$b_1(k_h, 0; \omega) = \left[ R_{01} + T_{01} R_{12} T_{10} e^{-iv_1(z_b - z_a)} \right] e^{-ik_z z_a} \delta(k_g - k_s), \quad (3.4)$$

or

$$b_1(k_h, 0; \omega) = \left[ R_{01} e^{-ik_z z_a} + R'_{12} e^{-iv_1(z_b - z_a)} e^{-ik_z z_a} \right] \delta(k_g - k_s), \quad (3.5)$$

where, for simplicity, we denoted  $T_{01} R_{12} T_{10} = R'_{12}$ .

For the first primary we can write (see Fig. 4(a))  $\cos\theta = q_s / (\omega / c_0)$  which implies

$$q_s = \frac{\omega}{c_0} \cos\theta \quad (3.6)$$

or, noticing that  $c_0 / \cos\theta = c_v^1$ , the vertical speed in the first medium,

$$q_s z_a = \frac{\omega}{c_0} z_a \cos\theta = \omega \frac{\tau^1}{2}, \quad (3.7)$$

where  $\tau^1$  represents the intercept or vertical time of the first event. Similarly, on the receiver side we have

$$q_g z_a = \omega \frac{\tau^1}{2}. \quad (3.8)$$

Summing the last two equations we find for the first primary arrival (compare with Eq. (2.17))

$$k_z z_a = \omega \tau^1, \quad (3.9)$$

where we emphasize again that on the left hand side of the equation is the reference  $k_z$  and the pseudo-depth, which in this case coincides with the actual depth of the reflector,  $z_a$ , and on the right hand side we have the phase information contained in the

recorded data. For the second event we can find, as before, that, for the portion propagating through the space in between the measurement surface and the depth  $z_a$ , we have

$$k_z z_a = \omega \tau_1, \quad (3.10)$$

where  $\tau_1$  is the vertical time through the first medium. For the part that is propagating through the second medium we can write  $\cos \varphi = q_{1s} / (\omega / c_1)$  which implies

$$q_{s1} = \frac{\omega}{c_1} \cos \varphi, \quad (3.11)$$

or, noticing that  $c_1 / \cos \varphi = c_v^2$ , the vertical speed in the layer,

$$q_{1s}(z_b - z_a) = \frac{\omega}{c_1} (z_b - z_a) \cos \varphi = \omega \frac{\tau_2}{2}, \quad (3.12)$$

where  $\tau_2$  is the vertical time through layer 2 for this event. Similarly, on the receiver side we have

$$q_{1g}(z_b - z_a) = \omega \frac{\tau_2}{2}. \quad (3.13)$$

Summing the last two equations we find

$$v_1(z_b - z_a) = \omega \tau_2. \quad (3.14)$$

Summarizing, for the second primary we found from Eqs. (3.10) and (3.14)

$$k_z z_a + v_1(z_b - z_a) = \omega \tau^2, \quad (3.15)$$

where  $\tau^2$  is the total vertical time for the second event.

Since the velocity of the second medium is not known, we can write  $\omega \tau^2$  in terms of  $c_0$  only as follows (see Eq. (2.17))

$$\omega \tau^2 = k_z z'_b, \quad (3.16)$$

where  $z'_b$  is a pseudo-depth which can be calculated in terms of the vertical time  $\tau^2$  and the vertical speed of the first medium. With these remarks, the expression (3.5) for  $b_1$  becomes

$$b_1(k_h, 0; \omega) = \left[ R_{01} e^{-ik_z z_a} + R'_{12} e^{-ik_z z'_b} \right] \delta(k_g - k_s). \quad (3.17)$$

To calculate  $b_1(k_h, z)$  we first downward continue/extrapolate,

$$b_1(k_h, z; \omega) = \left[ R_{01} e^{ik_z(z-z_a)} + R'_{12} e^{ik_z(z-z'_b)} \right] \delta(k_g - k_s), \quad (3.18)$$

and then integrate over  $k_z$  (imaging) to obtain

$$b_1(k_h, z) = \int_{-\infty}^{\infty} dk_z b_1(k_h, k_z; \omega). \quad (3.19)$$

Notice that the reflection and transmission coefficients in the expression (3.18) are functions of  $\omega$  and hence functions of  $k_z$ . Explicitly,

$$R_{01}(k_h, \omega) = \frac{\sqrt{\frac{4\omega^2}{c_0^2} - k_h^2} - \sqrt{\frac{4\omega^2}{c_1^2} - k_h^2}}{\sqrt{\frac{4\omega^2}{c_0^2} - k_h^2} + \sqrt{\frac{4\omega^2}{c_1^2} - k_h^2}}. \quad (3.20)$$

The integration over  $k_z$  in (3.19) hence amounts to an inverse Fourier transform of  $R_{01}$  and  $R'_{12}$  over  $k_z$ . This Fourier transform is difficult to write as an analytic result and hence the example can no longer continue in the  $(k_h, \omega)$  domain.

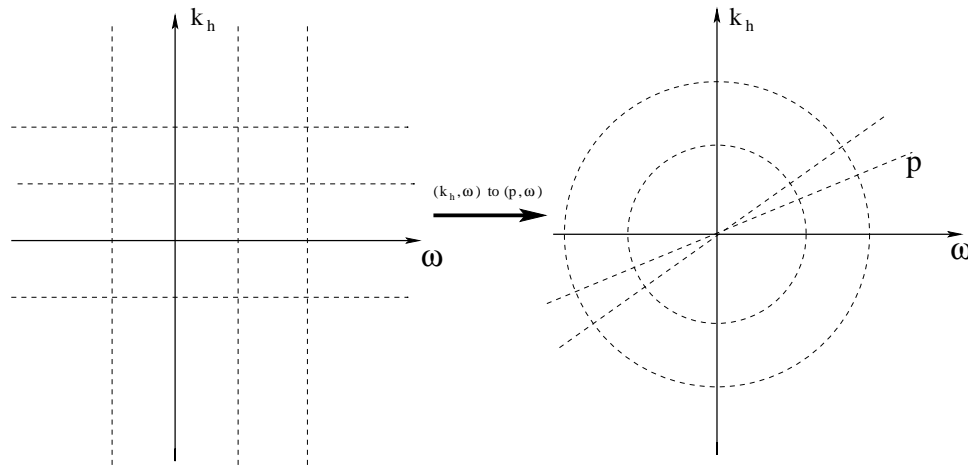


Figure 5: The mapping  $(k_h, \omega)$  to  $(p, \omega)$ .

The imaging of the data can also be achieved in the  $(p, \omega)$  domain with better analytical results and more meaningful amplitude analysis (see [5]). The slowness  $p$  is defined as the inverse of velocity,  $p = 1/c$ . To this end we map the data from the  $(k_h, \omega)$  to  $(p, \omega)$  domain. This mapping has been studied extensively in [3,4]. It mainly consists in reading the data along the lines going through the origin of the  $(k_h, \omega)$  coordinate system instead of the original  $(k_h, \omega)$  grid (see Fig. 5). Notice that, if this mapping is performed, the reflection and the transmission coefficients are no longer dependent of the frequency  $\omega$  or  $k_z$ . Explicitly, in the formula (3.20) for  $R_{01}$  we can factor  $\omega$  and then divide by it and so the expression becomes

$$R_{01}(p) = \frac{\sqrt{\frac{4}{c_0^2} - p^2} - \sqrt{\frac{4}{c_1^2} - p^2}}{\sqrt{\frac{4}{c_0^2} - p^2} + \sqrt{\frac{4}{c_1^2} - p^2}}. \quad (3.21)$$

Similarly it can be shown that  $R'_{12}$  is mapped to a function of  $p$  only.

In this new coordinate system the imaging step reads

$$b_1(p, z) = \int_{-\infty}^{\infty} dk_z b_1(p, k_z; \omega) = [R_{01}(p)\delta(z - z_a) + R'_{12}(p)\delta(z - z'_b)] \delta(k_g - k_s). \quad (3.22)$$

Numerical results comparing imaging in  $(k_h, \omega)$  and  $(p, \omega)$  were shown and discussed in [5]. The imaged data written in Eq. (3.22) is next taken through the internal multiple algorithm described in Eq. (2.10).

Given the data in the form (3.22), the algorithm performs similarly to the 1D normal incidence case. In the following, we are denoting by  $p_1, p_2$  and  $p_3$  the horizontal slowness associated with  $k_g + k_1, k_2 + k_s$  and  $k_1 + k_2$  respectively. The horizontal slowness associated with  $k_s + k_g$  is also denoted by  $p$ . The four slowness variables defined above are not independent, in fact we have that  $p_3 = (p_1 + p_2) - p$ .

The inner most integral towards calculating  $b_3$  in the internal multiple algorithm is

$$\begin{aligned} & \int_{z'_2 + \varepsilon_1}^{\infty} dz'_3 e^{ik_z z'_3} [R_{01}(p_2)\delta(z'_3 - z_a) + R'_{12}(p_2)\delta(z'_3 - z'_b)] \delta(k_2 - k_s) \\ &= \int_{-\infty}^{\infty} dz'_3 H(z'_3 - (z'_2 + \varepsilon_1)) e^{ik_z z'_3} [R_{01}(p_2)\delta(z'_3 - z_a) + R'_{12}(p_2)\delta(z'_3 - z'_b)] \delta(k_2 - k_s) \\ &= [H(z_a - (z'_2 + \varepsilon_1))R_{01}(p_2)e^{ik_z z_a} + H(z'_b - (z'_2 + \varepsilon_1))R'_{12}(p_2)e^{ik_z z'_b}] \delta(k_2 - k_s). \end{aligned} \quad (3.23)$$

The second integral in the algorithm is

$$\begin{aligned} & \int_{-\infty}^{z'_1 - \varepsilon_2} dz'_2 e^{ik_z z'_2} [R_{01}(p_3)\delta(z'_2 - z_a) + R'_{12}(p_3)\delta(z'_2 - z'_b)] \delta(k_1 - k_2) \\ & \quad \times [H(z_a - (z'_2 + \varepsilon_1))R_{01}(p_2)e^{ik_z z_a} + H(z'_b - (z'_2 + \varepsilon_1))R'_{12}(p_2)e^{ik_z z'_b}] \delta(k_2 - k_s) \\ &= R_{01}(p_2)R_{01}(p_3)H((z'_1 - \varepsilon_2) - z_a)\underline{H(z_a - (z_a + \varepsilon_1))}e^{ik_z z_a}e^{-ik_z z_a}\delta_{12s} \\ & \quad + R_{01}(p_3)R'_{12}(p_2)H((z'_1 - \varepsilon_2) - z_a)H(z'_b - (z_a + \varepsilon_1))e^{ik_z z'_b}e^{-ik_z z_a}\delta_{12s} \\ & \quad + R'_{12}(p_3)R_{01}(p_2)H((z'_1 - \varepsilon_2) - z'_b)\underline{H(z_a - (z'_b + \varepsilon_1))}e^{ik_z z_a}e^{-ik_z z'_b}\delta_{12s} \\ & \quad + R'_{12}(p_2)R'_{12}(p_3)H((z'_1 - \varepsilon_2) - z'_b)\underline{H(z'_b - (z'_b + \varepsilon_1))}e^{ik_z z'_b}e^{-ik_z z'_b}\delta_{12s}, \end{aligned} \quad (3.24)$$

where

$$\delta_{12s} = \delta(k_1 - k_2)\delta(k_2 - k_s)$$

and all the underlined terms are zero.

The last integral over depth  $z$  in the calculation of  $b_3$  is

$$\begin{aligned}
& \int_{-\infty}^{\infty} e^{ik_z z'_1} [R_{01}(p_1)\delta(z'_1 - z_a) + R'_{12}(p_1)\delta(z'_1 - z'_b)] \delta(k_g - k_1) \\
& \quad \times R_{01}(p_2)R'_{12}(p_3)H((z'_1 - \varepsilon_2) - z_a)H(z'_b - (z_a + \varepsilon_1))e^{ik_z z'_b} e^{-ik_z z_a} \delta_{12s} \\
& = R_{01}(p_1)R_{01}(p_2)R'_{12}(p_3)\underline{H(-\varepsilon_2)}H(z'_b - (z_a + \varepsilon_1))e^{ik_z z_a} \delta(k_g - k_1)\delta_{12s} \\
& \quad + R'_{12}(p_1)R_{01}(p_2)R'_{12}(p_3)e^{ik_z(2z'_b - z_a)}H(z'_b - (z_a + \varepsilon_2))H(z'_b - (z_a + \varepsilon_1))\delta(k_g - k_1)\delta_{12s} \\
& = R'_{12}(p_1)R_{01}(p_2)R'_{12}(p_3)e^{2ik_z z'_b} e^{-ik_z z_a} \delta(k_g - k_1)\delta_{12s}, \tag{3.25}
\end{aligned}$$

where we have used the fact that the underlined term is zero and that the last two Heaviside functions are identically equal to 1.

The result for the  $b_3$ , and hence the predicted first order internal multiple, is

$$b_3(p, \omega) = e^{2ik_z z'_b} e^{-ik_z z_a} \int_{-\infty}^{\infty} dk_1 \int_{-\infty}^{\infty} dk_2 R'_{12}(p_1)R_{01}(p_2)R'_{12}(p_3)\delta(k_g - k_1)\delta_{12s}, \tag{3.26}$$

or, after evaluating the integrals and using the relationship between  $p_1$ ,  $p_2$ ,  $p_3$  and  $p$ ,

$$b_3(p, \omega) = R_{12}^2(p)R_{01}(p)\delta(k_g - k_s)e^{2ik_z z'_b} e^{-ik_z z_a}. \tag{3.27}$$

Recalling that  $R_{12}^2(p) = T_{01}(p)R_2(p)T_{10}(p)$  we find the final result to be

$$b_3(p, \omega) = T_{01}^2(p)R_2^2(p)T_{10}^2(p)R_{01}(p)\delta(k_g - k_s)e^{2ik_z z'_b} e^{-ik_z z_a} \tag{3.28}$$

consistent with the 1D normal incident result of [18]. Integrating over  $k_h$  gives the prediction of the first order internal multiple in space frequency domain

$$IM_{predicted}^{1st}(x_h, 0; \omega) = \frac{1}{2\pi} \int_{-\infty}^{\infty} dk_h \frac{T_{01}^2 R_{12}^2 T_{10}^2 R_{10} e^{2iv_1(z_b - z_a)}}{iq_s} e^{ik_h x_h} e^{ik_z z_a}. \tag{3.29}$$

Comparing this expression with Eq. (3.2) for the actual multiple we see that the predicted multiple has the correct total time and a well approximated amplitude. The amplitude of the predicted multiple in the  $p$ -domain is within a  $T_{01}(p)T_{10}(p)$  factor, a factor which is always close to, but always less than, 1. An integration over the horizontal wavenumber  $k_h$  will average these amplitudes and will result in the predicted amplitude in the space domain which again is going to be lower than, but close to, the actual amplitude of the internal multiple. In addition, since the phase and amplitude construction is performed in the plane waves domain, the internal multiples with headwaves sub-events are also predicted by the algorithm.

In the next section we will further discuss the lower-higher-lower relationship between the pseudo-depths of the sub-events and the similarities and differences of this relationship in total travel time and vertical or intercept time.

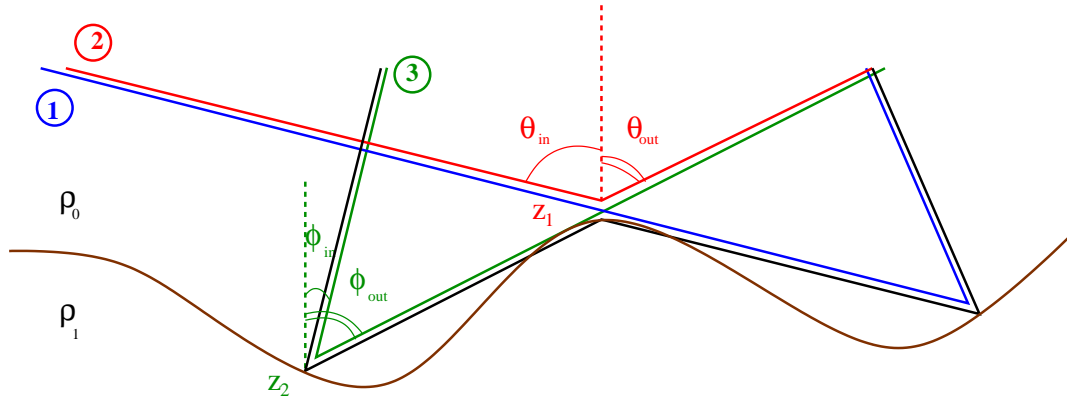


Figure 6: A 2D model with internal multiple reflections satisfying the time monotonicity in the vertical time but not in the total travel time.

#### 4 Vertical time and total travel time monotonicity: A 2D example

Consider the model shown in Fig. 6. For simplicity we assume that only the density  $\rho$  varies at the interface and it has the value  $\rho_0$  in the reference medium and  $\rho_1$  in the actual medium. The velocity is constant  $c_0$ . In this picture, the sub-events in the data which determine the internal multiple are numbered 1, 2 and 3; the actual internal multiple (the W shaped event) predicted by these sub-events is shown without any number.

First, notice that, we can find a depth for the sources and receivers such that the total traveltimes of the shallower reflection (event number 2) is larger than both deeper reflections (1 and 3). This is due to the large offsets needed to record such a large offset event. This implies that the longer-shorter-longer relationship is not satisfied by these particular sub-events in the total traveltime.

Next we calculate the vertical times for individual sub-events. The vertical time for the event 2 along the left leg is (see Fig. 6)

$$\tau_2^1 = z_1 \frac{\cos\theta_{in}}{c_0}, \quad (4.1)$$

where the subscript indicates the event number and the superscript indicating that it is the first part (left leg) of the total vertical time  $\tau$ ; along the right leg we have

$$\tau_2^2 = z_1 \frac{\cos\theta_{out}}{c_0}. \quad (4.2)$$

Summing the two legs we find the total vertical time along the event 2 to be

$$\tau_{red} = \frac{z_1}{c_0} (\cos\theta_{in} + \cos\theta_{out}). \quad (4.3)$$

Similarly, for event 3, we have

$$\tau_3 = \frac{z_2}{c_0} (\cos\phi_{in} + \cos\phi_{out}). \quad (4.4)$$

Since the velocity is constant,  $\theta_{out} = \phi_{out}$ ; we also have that  $\phi_{in} < \theta_{in}$ , and hence  $\cos\phi_{in} > \cos\theta_{in}$ , and  $z_2 > z_1$  which results in

$$\tau_3 > \tau_2. \quad (4.5)$$

It is not difficult to see that similarly, for this example, we have

$$\tau_1 > \tau_2 \quad (4.6)$$

where  $\tau_1$  is the vertical time of primary reflection 1 in Fig. 6.

The conclusion is that for this model and particular internal multiple, the longer-shorter-longer relationship is satisfied by the vertical or intercept times of the three subevents but not by their total traveltimes. According to Eq. (2.17), this relation translates into the lower-higher-lower relationship between the pseudo-depths of the subevents and hence the internal multiple depicted in Fig. 6 will be predicted by the inverse scattering internal multiple attenuation algorithm in Eq. (2.10).

In the next section we discuss a model and a particular type of internal multiples for which the longer-shorter-longer relationship in vertical and total travel time is not satisfied.

## 5 Breaking the time monotonicity: A 2D example

Consider the model shown in Fig. 7 where  $c_0 < c_1$  (a similar example was discussed by ten Kroode [8]). A high velocity zone, in which the propagation speed is  $c_3$  much higher than  $c_0$ , intersects one leg of the internal multiple and hence one leg of one of the subevents (one of the single reflection in Fig. 7). Due to this high velocity zone and the fact that  $c_0 < c_1$ , one can easily imagine a situation in which both the total and the vertical time of the deeper single reflection passing through the high velocity zone are shorter than the total and vertical times respectively of the shallow single reflection. In this case the lower-higher-lower relationship between the pseudo-depths of the sub-events is not satisfied and hence the internal multiple shown in the picture will not be predicted. The monotonicity is in consequence broken, since even though the actual depths still satisfy a lower-higher-lower relationship, the pseudo-depths, vertical times or total times of the sub-events do not.

To better understand the multiples which do not satisfy the pseudo-depth/vertical-time monotonicity condition and to expand the algorithm to address them, one has to study their creation in the forward scattering series. As indicated by Matson in [10, 11] and Weglein et al. [18] the lower-higher-lower relationship in pseudo-depth  $z$  was pointed to by the forward scattering series: the first order approximation to an internal multiple is constructed in the forward scattering series from interactions with point scatterers which satisfy the lower-higher-lower relationship in actual depth. It would be interesting to analyze how a multiple that breaks the monotonicity assumption is constructed by the forward series and to determine if an analogy between the forward and

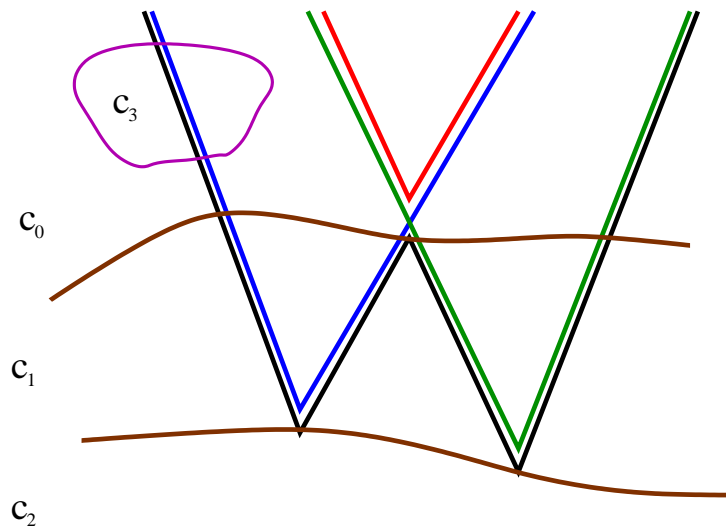


Figure 7: A 2D model with an internal multiple containing sub-events which do not satisfy the time monotonicity in either total travelttime or vertical time.

the inverse process would be useful to expand the algorithm to address these kind of events. This particular issue and others will be the subject of future research.

## 6 Conclusions

In this paper we presented an analysis of the inverse scattering algorithm for attenuating internal multiple reflections. We particularly focused on the mechanism of predicting amplitude and phase properties of such a wave event. We have presented the first application of the algorithm to analytical data in 1.5D (a 1D medium with the wavefield propagating in 2D) which shows the ability of the algorithm to exactly predict the time and well approximate the amplitude of internal multiple reflections, including the ones with headwaves sub-events. We have discussed in detail the pseudo-depth/vertical-time monotonicity condition and compared it with a similar total travel time relation. Furthermore, we showed that this restriction on the sub-events can be too strong and could prevent the prediction of some complex internal multiples.

This research is an important step forward in better understanding the inverse scattering series and, more specifically, the internal multiple attenuation algorithm derived from it. The analytic and qualitative analysis presented, targets internal multiples which occur in complex and higher dimensional media. Having a better understanding of the structure and definition of such internal multiples opens up new possibilities of identifying, predicting and subtracting them from the collected data. The inverse scattering series is presently the only tool that can achieve these objectives without any knowledge about the actual medium.

## Acknowledgments

This work was partially supported by NSF-CMG award number DMS-0327778 and the DOE Basic Energy Sciences award DE-FG02-05ER15697. The support of M-OSRP sponsors is also gratefully acknowledged. Adriana C. Ramírez is thanked for providing the model in Fig. 6. Jon Sheiman, Einar Otnes and Fons ten Kroode are acknowledged for their useful comments and insights on this work.

## References

- [1] K. AKI, P. G. RICHARDS (1980), *Quantitative Seismology*, W. H. Freeman and Company, San Francisco.
- [2] F. V. ARAUJO (1956), *Linear and Nonlinear Methods Derived from Scattering Theory: Backscattered Tomography and Internal Multiple Attenuation*, Ph.D. thesis, Department of Geophysics, Universidad Federal de Bahia, Salvador-Bahia, Brazil, 1994 (in Portuguese).
- [3] R. N. BRACEWELL (1956), *Strip integration in radio astronomy*, Aust. J. Phys., Vol. 9, pp. 198-217.
- [4] R. N. BRACEWELL, A. C. RIDDLE (1967), *Inversion of fan-beam scans in radio astronomy*, Astrophys. J., Vol. 150, pp. 427-434.
- [5] C. G. M. BRUIN, C. P. A. WAPENAAR, A. J. BERKHOUT (1990), *Angle-dependent reflectivity by means of prestack migration*, Geophysics, Vol. 55, No. 9, pp. 1223-1234.
- [6] P. M. CARVALHO (1992), *Free Surface Multiple Reflection Elimination Method Based on Nonlinear Inversion of Seismic Data*, Ph.D. thesis, Department of Geophysics, Universidad Federal de Bahia, Salvador-Bahia, Brazil, (in Portuguese).
- [7] J. B. DIEBOLD AND P. L. STOFFA (1981), *The travelttime equation, tau-p mapping, and inversion of common midpoint data*, Geophysics, Vol. 46, No. 3, pp. 238-254.
- [8] F. TEN KROODE (2002), *Prediction of internal multiples*, Wave Motion, Volume 35, No. 4, pp. 315-338.
- [9] A. MALCOLM AND M. V. DE HOOP (2005), *A method for inverse scattering based on the generalized Bremmer coupling series*, Inverse Problems, Vol. 21, pp. 1137-1167.
- [10] K. H. MATSON (1996), *The relationship between scattering theory and the primaries and multiples of reflection seismic data*, J. Seismic Exploration, 5, pp. 63-78.
- [11] K. H. MATSON, *An Inverse Scattering Series Method for Attenuating Elastic Multiples from Multicomponent Land and Ocean Bottom Seismic Data*, Ph.D. thesis, Department of Earth and Ocean Sciences, University of British Columbia, Vancouver, BC, Canada, 1997.
- [12] B. G. NITA AND A. B. WEGLEIN (2004), *Imaging with  $\tau = 0$  versus  $t = 0$ : implications for the inverse scattering internal multiple attenuation algorithm*, SEG Expanded Abstracts, 74<sup>th</sup> Annual Meeting of the Society for Exploration Geophysicists, Denver, Colorado.
- [13] R. STOLT (1978), *Migration by Fourier transform*, Geophysics, 43, pp. 23-48.
- [14] R. STOLT AND A. B. WEGLEIN (1985), *Migration and inversion of seismic data*, Geophysics, 50, pp. 2458-2472.
- [15] J. R. TAYLOR, *Scattering Theory*, John Wiley and Sons, New York, 1972.
- [16] S. TREITEL, P. R. GUTOWSKI AND D. E. WAGNER (1982), *Plane-wave decomposition of seismograms*, Geophysics, Vol. 47, No. 10, pp. 1374-1401.

- [17] A. B. WEGLEIN, F. A. GASPAROTTO, P. M. CARVALHO, R. H. STOLT (1997), *An inverse scattering series method for attenuating multiples in seismic reflection data*, *Geophysics*, 62, pp. 1975-1989.
- [18] A. B. WEGLEIN, F. V. ARAUJO, P. M. CARVALHO, R. H. STOLT, K. H. MATSON, R. COATES, D. CORRIGAN, D. J. FOSTER, S. A. SHAW, H. ZHANG (2003), *Inverse scattering series and seismic exploration*, *Topical Review Inverse Problems*, 19, pp. R27-R83.
- [19] A. B. WEGLEIN, W. DRAGOSET (2005), editors for *Internal Multiples*, SEG Reprint Volume.